

Organic & Biomolecular Chemistry

Accepted Manuscript



This is an *Accepted Manuscript*, which has been through the Royal Society of Chemistry peer review process and has been accepted for publication.

Accepted Manuscripts are published online shortly after acceptance, before technical editing, formatting and proof reading. Using this free service, authors can make their results available to the community, in citable form, before we publish the edited article. We will replace this *Accepted Manuscript* with the edited and formatted *Advance Article* as soon as it is available.

You can find more information about *Accepted Manuscripts* in the [Information for Authors](#).

Please note that technical editing may introduce minor changes to the text and/or graphics, which may alter content. The journal's standard [Terms & Conditions](#) and the [Ethical guidelines](#) still apply. In no event shall the Royal Society of Chemistry be held responsible for any errors or omissions in this *Accepted Manuscript* or any consequences arising from the use of any information it contains.



Organic & Biomolecular Chemistry

ARTICLE

Synthesis of 2-deoxy-2,2-difluoro- α -maltosyl fluoride and its X-ray structure in complex with *Streptomyces coelicolor* GlgEI-V279S

Received 00th January 20xx,
Accepted 00th January 20xx

DOI: 10.1039/x0xx00000x

www.rsc.org/

Sandeep Thanna^{†a}, Jared J. Lindenberger^{†a}, Vishwanath V. Gaitonde^a, Donald R. Ronning^{*a} and Steven J. Sucheck^{*a}

Streptomyces coelicolor (Sco) GlgEI is a glycoside hydrolase involved in α -glucan biosynthesis and can be used as a model enzyme for structure-based inhibitor design targeting *Mycobacterium tuberculosis* (Mtb) GlgE. The latter is a genetically validated drug target for the development of anti-Tuberculosis (TB) treatments. Inhibition of Mtb GlgE results in a lethal buildup of the GlgE substrate maltose-1-phosphate (M1P). However, Mtb GlgE is difficult to crystallize and affords lower resolution X-ray structures. Sco GlgEI-V279S on the other hand crystallizes readily, produces high resolution X-ray data, and has active site topology identical to Mtb GlgE. We report the X-ray structure of Sco GlgEI-V279S in complex with 2-deoxy-2,2-difluoro- α -maltosyl fluoride (α -MTF, **5**) at 2.3 Å resolution. α -MTF was designed as a non-hydrolysable mimic of M1P to probe the active site of GlgEI prior to covalent bond formation without disruption of catalytic residues. The α -MTF complex revealed hydrogen bonding between Glu423 and the C1'F which provides evidence that Glu423 functions as proton donor during catalysis. Further, hydrogen bonding between Arg392 and the axial C2' difluoromethylene moiety of α -MTF was observed suggesting that the C2' position tolerates substitution with hydrogen bond acceptors. The key step in the synthesis of α -MDF was transformation of peracetylated 2-fluoro-maltal **1** into peracetylated 2,2-difluoro- α -maltosyl fluoride **2** in a single step via the use of Selectfluor[®]

Introduction

Tuberculosis (TB) is an epidemic disease caused by the *Mycobacterium tuberculosis* (Mtb) complex. According to the World Health Organization¹, TB resulted in the death of 1.5 million people from a total of 9.0 million infection cases in 2013. Of those cases, multidrug-resistant TB (MDR-TB) is estimated to represent half a million cases and the actual number of MDR-TB cases diagnosed has tripled between 2009 and 2013. An estimated 9% of people with MDR-TB have TB classified as extensively drug-resistant TB (XDR-TB). The treatment regimens for these differing forms of TB are highly complex and there are five classes of drug groups used to treat TB². The common first line drugs are classified as Group 1. Oral and include: isoniazid (H/Inh), rifampicin/rifampin (R/Rif), pyrazinamide (Z/Pza), ethambutol (E/Emb), rifapentine (P/Rpt) or rifabutin (Rfb). The current standard for treating drug sensitive TB involves a quadruple drug combination: two months of four drugs (Inh, Rif, Pza and Emb) in the intensive phase followed by four months of Inh plus Rif in the continuation stage. It is commonly believed that resistance develops during these long treatment times thereby requiring

the use of second and third line TB drugs. Thus, there is a great need to identify drugs for treating drug-resistant and drug-sensitive TB in a shorter time span.

Mtb GlgE is an essential enzyme which catalyzes the synthesis of cytoplasmic α -glucan by transferring maltose-1-phosphate (M1P) (Fig. 1) to a growing α -1,4-glucan chain. The pathway begins with isomerization of trehalose by TreS into maltose. The latter is phosphorylated by Pep2 kinase to form maltose-1-phosphate (M1P) which is utilized by GlgE to produce linear α -1,4-glucan. Inhibiting GlgE results in accumulation of M1P which causes rapid death of Mtb in vitro and in mice³. We have reported the first inhibitors of Mtb GlgE. These include maltose-C-phosphonate (MCP)⁴ and 2,5-dideoxy-3-O- α -D-glucopyranosyl-2,5-imino-D-mannitol⁵ designed as substrate and transition state inhibitors,

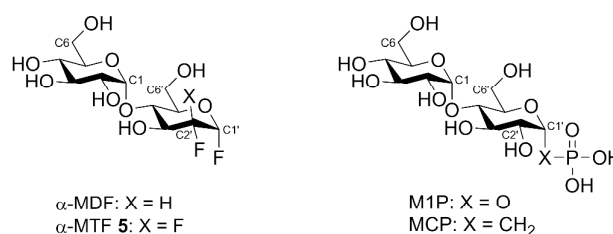


Fig. 1 Mimics of M1P. 2-Deoxy-2-fluoro- α -maltosyl fluoride (α -MDF), 2-deoxy-2,2-difluoro- α -maltosyl fluoride (α -MTF, **5**), and MCP. Numbering for selected carbon atoms is indicated.

^a Department of Chemistry and Biochemistry, The University of Toledo, 2801 W. Bancroft Street, MS602, Toledo, OH, USA 43606. E-mail: donald.ronning@utoledo.edu; steve.sucheck@utoledo.edu

[†] S.T. and J.J.L. contributed equally to the manuscript.

Electronic Supplementary Information (ESI) available: [¹H and ¹³C NMR spectra for compounds are available, PDB ID Code: 4U2Z]. See DOI: 10.1039/x0xx00000x

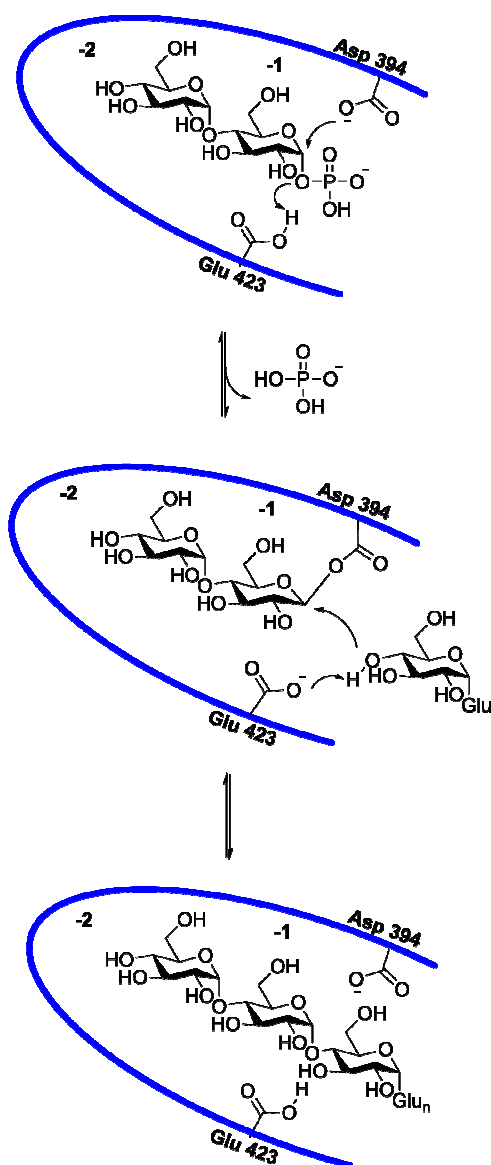
respectively. To identify more potent inhibitors we have embarked on a structure-based inhibitor study which utilizes X-ray crystallography to reveal key binding interactions between GlgE and our target ligands. We anticipate these studies will inform improved inhibitor designs. However, an obstacle to achieving this goal is that *Mtb* GlgE crystallizes poorly/slowly and crystals diffract to afford lower resolution X-ray data (e.g. 3.2 – 4.0 Å)⁶. To obtain X-ray structures with higher throughput and resolution, *Sco* GlgEI-V279S was designed as a readily crystallized homologue of *Mtb* GlgE that possesses the same active site topology as *Mtb* GlgE⁶. This approach has been highly successful and has generated X-ray complexes of both MCP and 2,5-dideoxy-3-*O*- α -D-glucopyranosyl-2,5-imino-D-mannitol⁶, and now, 2-deoxy-2,2-difluoro- α -maltosyl fluoride (α -MTF, **5**) (Fig. 1) at 2.3 Å resolution.

GlgE catalyzes the transfer of a maltose unit onto a growing α -glucan using an α -retaining double-displacement mechanism⁷. Using the *Sco* GlgEI numbering, Asp394 acts as the initial nucleophile acting on M1P forming a β -maltosyl enzyme intermediate (Scheme 1). Glu423 also participates in this reaction by donating a proton to the leaving oxygen atom. The resulting β -maltosyl enzyme intermediate is attacked by the 4-OH at the non-reducing end of an α -glucan chain to extend the chain by a maltose unit (two glucose units). In this reaction, it is predicted that Glu423 acts as a general base to deprotonate the acceptor hydroxyl of the incoming α -glucan. Recently, 2-deoxy-2-fluoro- α -maltosyl fluoride (α -MDF), (Fig. 1) has been reported to trap the maltosyl-enzyme intermediate of a general base-inactivated *Sco* GlgEI-E423A variant enzyme⁸. That study is notable as the E423A point mutation was required to prevent hydrolysis of the β -maltosyl enzyme intermediate. In the structure described here, *Sco* GlgEI-V279S contains the general base Glu423 and yet α -MTF co-crystallized with enzyme fully intact and showed no formation of a covalent glycosyl-enzyme intermediate. Based on previously reported studies involving homologous 2-deoxy-2,2-difluoroglycosides^{9,10}, the lower reactivity of the trifluoride **5** can be most readily explained by reactivity differences that result from the lower leaving group ability of the C1' fluorine. Analysis of the X-ray complex and comparison with the complementary MCP probe reveals the hydrogen bonding interactions present within the inhibitor-enzyme complex just prior to formation of the glycosyl enzyme intermediate. Comparison of these structures also reveals the role of the M1P phosphate in orienting the -1 site sugar into a reactive geometry. We also outline a synthesis of α -MTF (**5**) which was accessed from peracetylated 2,2-difluoro- α -maltosyl fluoride **2**. These targets were accessed in a single step, via the use of Selectfluor[®] on peracetylated 2-fluoro-maltal **1**¹⁰.

Results and discussion

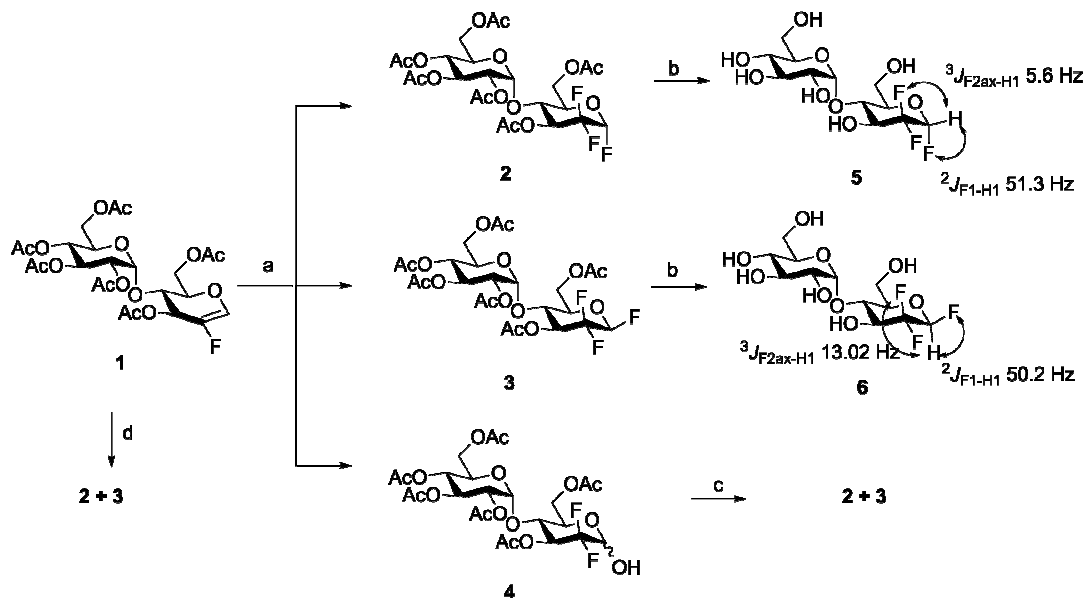
Synthesis of 2,2-difluoro- α/β -D-maltosyl fluorides (**2**, **3**)

2-Deoxy-2,2-difluoro- α/β -maltosyl fluorides were accessed from the peracetylated 2-fluoro-maltal **1**,¹⁰ (Supporting



Scheme 1. Catalytic mechanism of α -retaining glycoside hydrolase *Sco* GlgEI. Glu_n = α -1,4-glucose polymer.^{7,8} The blue line represents the enzyme active site and the -2 and -1 represent the sugar-binding subsite nomenclature.

Information, Scheme S-1). Subsequently, peracetylated 2,2-difluoro- α -maltosyl fluoride **2** and peracetylated 2,2-difluoro- β -maltosyl fluoride **3** were prepared by one of three routes. One route was by the direct conversion of peracetylated 2-fluoro-maltal **1** into **2** and **3** with Selectfluor[®] in dry nitromethane in single step as shown in Scheme 2.¹¹ This also produced a small amount of an anomeric mixture of 2,2-difluoro maltose hemiacetal **4**. The combined yield of the reaction was 61.3% to access **2** + **3** + **4** (ratio 21.3:18.5:21). Treatment of hemiacetal **4** with diethylaminosulfur trifluoride (DAST) also yielded a mixture of **2** and **3**.¹¹ This reaction was slow and afforded moderate yields. In another condition, peracetylated 2-fluoro-maltal **1** was treated with XeF₂ in CCl₃



Scheme 2. Synthesis of 2-deoxy-2,2-difluoro-(α/β)-maltosyl fluorides **5** and **6**. Reagents and conditions: a) Selectfluor[®], dry CH₃NO₂ (**2** + **3** + **4** combined 61%); b) NH₃-MeOH, quantitative; c) DAST, dry CH₂Cl₂ (**2** + **3** combined 17%); d). XeF₂, CFCl₃ (12%). The anomeric configuration of **5** and **6** was determined by ¹H NMR based on H-F coupling constants indicated.

at -20 °C to afford an α/β mixture of peracetylated 2,2-difluoromaltosyl fluorides with a modest 12% yield. Glycosides **2** and **3** were deprotected by using NH₃-methanol to afford 2-deoxy-2,2-difluoro- α -maltosyl fluoride (**5**) and 2-deoxy-2,2-difluoro- β -maltosyl fluoride (**6**), respectively. The anomeric configuration was assigned by the H-F coupling constants as shown in Scheme 2.

Enzyme inhibition assay of α -MTF

Recombinant *Sco* GlgE1-V279S is produced in *E. coli* and purified using the methods detailed previously⁵. Inhibition of this enzyme using **2** α -MTF (**5**) and 2-deoxy-2,2-difluoro- β -maltosyl fluoride (**6**) was performed by coupling GlgE1-V279S activity with the commercially available EnzCheck[®] Phosphate Assay Kit (Life Technologies)⁴. The compounds showed no inhibitory activity below 10 mM concentration.

Enzyme substrate assay for α -MTF

As an orthogonal qualitative assessment, MALDI-MS was performed to evaluate α -MTF incorporation into maltooligosaccharides via *Sco* GlgE-V279S and compared to a series of controls (Fig S-1, Supporting Information,). The results indicate α -MTF was not a substrate for GlgE.

X-ray crystal structure of the *Sco* GlgE1-V279S- α -MTF complex

A complex of *Sco* GlgE1-V279S and α -MTF was co-crystallized and the structure solved using the *Sco* GlgE-V279S-MCP structure as a model for rigid body refinement (RCSB ascension number 4U31), Table 1. Inspection of the initial |F_o-F_c| map exhibited clear density for the maltosyl unit of the α -MTF (Fig

2A), but no continuous density was observed between the nucleophile, Asp394, and the α -MTF, indicating the absence of a covalent intermediate. NMR and mass spectrometry experiments produced negative results for the GlgE1-V279S catalyzed transfer reaction using α -MTF, which suggests that *Sco* GlgE1-V279S cannot undergo a nucleophilic attack on α -MTF. Difference density is observed for the 2,2-difluoromethylene group at C2' with the final model exhibiting a pair of hydrogen bonded interactions between the difluoromethylene moiety and the side chain of Arg392 (Fig 2B and 2C). The nucleophile Asp394 is forming a non-covalent bond with the equatorial fluorine at C2'. This suggests that Asp394 may be protonated in this form. Considering the role of Asp394 as a nucleophile in the catalytic reaction, an intriguing alternative interpretation is that this interaction may represent a halogen bond between the carboxylate of Asp394 and the fluorine at C2'.

Residue Glu423, proposed to function as a general acid to protonate the phosphate leaving group, is forming a 3.3 Å hydrogen bond with atom F1 since it is expected to be protonated during the first step of catalysis. Similar to the case of the interaction between Asp394 and the fluorine at C2', the protonation state of Glu423 is unknown and the interaction with F1 may represent a halogen bond. Additionally, interactions observed between the protein and the second glucosyl moiety of the α -MTF are consistent with those observed in other GlgE structures (not shown).

After preparing α -MTF we evaluated its ability to serve as a substrate for *Sco* GlgE1-V279S. We found, in the absence of a maltosyl-donor *Sco* GlgE1-V279S is able hydrolyze maltooligosaccharides and rearrange them into both longer

Table 1. X-ray crystallographic data collection and refinement statistics for *Sco* GlgEIV279S- α -MTF. The necessary data were obtained from one crystal. Values in parentheses are for the highest shells.

<i>Sco</i> GlgEIV279S- α -MTF complex	
Data collection	
Wavelength (Å)	1.08
Space group	P4 ₁ 2 ₁ 2
Cell dimensions	
<i>a</i>	113.3 Å
<i>b</i>	113.3 Å
<i>c</i>	314.3 Å
α	90°
β	90°
γ	90°
Resolution (Å)	50.0 – 2.3
<i>R</i> _{merge}	10.0 (51.0)
<i>I</i> / σ	26.0 (4.1)
Completeness (%)	99.9 (100)
Redundancy	8.3 (8.3)
Refinement	
Resolution (Å)	42.6 – 2.3
No. unique reflections	96,584
<i>R</i> _{work} / <i>R</i> _{free}	0.1629/0.1993
No. atoms	
Protein	10276
Ligand/ion	48
Water	891
B-factors (Å ²)	
Protein	35.9
Ligand/ion	37.0
Water	38.3
R.m.s deviations	
Bond lengths (Å)	0.008
Bond angles (°)	1.08
Ramachandran	
Favored (%)	97.7
Outliers (%)	0.1

and shorter polymers via a maltosyl-mixing (transglycosylation) process⁷. That reaction was performed, as a control, in order to determine the relative abundance of certain maltooligosaccharide sizes that would be observed if α -MTF could *not* be utilized as a substrate. A variety of maltooligosaccharide sizes were observed from the smallest four maltose units (M4), up to the largest twelve maltose units (M12) (Fig S-1B, Supporting Information). The relative intensities suggest that the *Sco* GlgE-V279S prefers chain lengths of six maltose units (M6) and eight maltose units (M8) (~2:1 ratio) as acceptors rather than the larger maltooligosaccharides such as ten maltose units (M10) (~7:1) and twelve maltose units (M12) (~66:1). The production of M4, which appears in an approximate ratio of 12:1 with M6, is likely the result of the hydrolysis of a maltosyl unit from the M6.

It had been shown previously that that M1F could be used as an efficient maltosyl-donor for both the wild-type *Mtb* and *Sco* GlgE⁷. Therefore, this glycosyl fluoride was used as a control substrate for these tests (Fig S-1, Supporting Information). Using the M1F as a donor substrate results in a mass increase of 320 Daltons. The relative ratios of the maltooligosaccharides compared to the M6 changed significantly compared to the control reaction of the *Sco*GlgE-V279S and M6 (Fig S-1C, Supporting Information). Significantly more M8 was produced (~1.1:1) in addition to M10 (~3:1) and M12 (10:1). Again, some M4 was produced (~14:1 in slightly lower amounts than the control, and is likely the result of the background maltosyl-mixing process observed in the control reactions performed without M1F. In addition, M14 was produced (~59:1), which did not occur in the control reaction. Whereas the control reaction represented the maltosyl mixing process, the reaction with the M1F maltosyl donor suggests authentic elongation of the polysaccharide.

Any maltooligosaccharides generated by the incorporation of the α -MTF would result in a mass increase of approximately 344 Daltons per unit as a result of the presence of the difluoro substitution at C2'. This is in contrast to the M1F, where an addition would change the mass by 324 Daltons; the incorporation of single maltosyl unit from the M1F. Reactions using the α -MTF as a substrate do not show incorporation of difluoride into M6 (Fig S-1D, Supporting Information). The spectrum observed from the α -MTF reaction is characteristic of the control reaction containing only M6 and GlgE. Indeed, the observed ion ratios are similar to that observed in the M6 control reaction further suggesting that the α -MTF also does not inhibit the maltosyltransfer reaction. However, most obvious, is the lack of the additional 20 Daltons that would accompany either the incorporation of the α -MTF via elongation or as a result of maltosyl-mixing. Taken together, these data suggest that the α -MTF cannot be used as a maltosyl-donor for GlgE activity and does not inhibit the activity of GlgE either.

The structure of the *Sco* GlgE-E423A covalently modified using α -MDF was recently published showing that 2-deoxy-2-fluoroglycosyl fluorides react with this general base-inactivated variant enzyme⁸. In an attempt to form a stable non-covalent complex with a fully active enzyme, we crystallized a complex of chimeric *Sco* GlgE-V279S with α -MTF. In contrast to the α -MDF, the α -MTF complex structure described here lacks contiguous difference density between the Asp394 nucleophile and α -MTF, suggesting that α -MTF has not undergone nucleophilic attack by the enzyme. This is likely the result of the difluoromethylene center at the C2' position being highly electron withdrawing and thus strongly destabilizing the putative oxocarbenium transition state and making the fluorine at C1' a very poor leaving group and thereby inhibiting the enzymatic reaction. This result suggests that α -MTF, and perhaps other 2-deoxy-2,2-difluoro-glycosyl fluorides, can be used as non-hydrolysable substrate analogues for glycoside hydrolases. Therefore, the *Sco* GlgE-V279S- α -MTF complex can be used to infer key molecular interactions between authentic substrate and GlgE-V279S

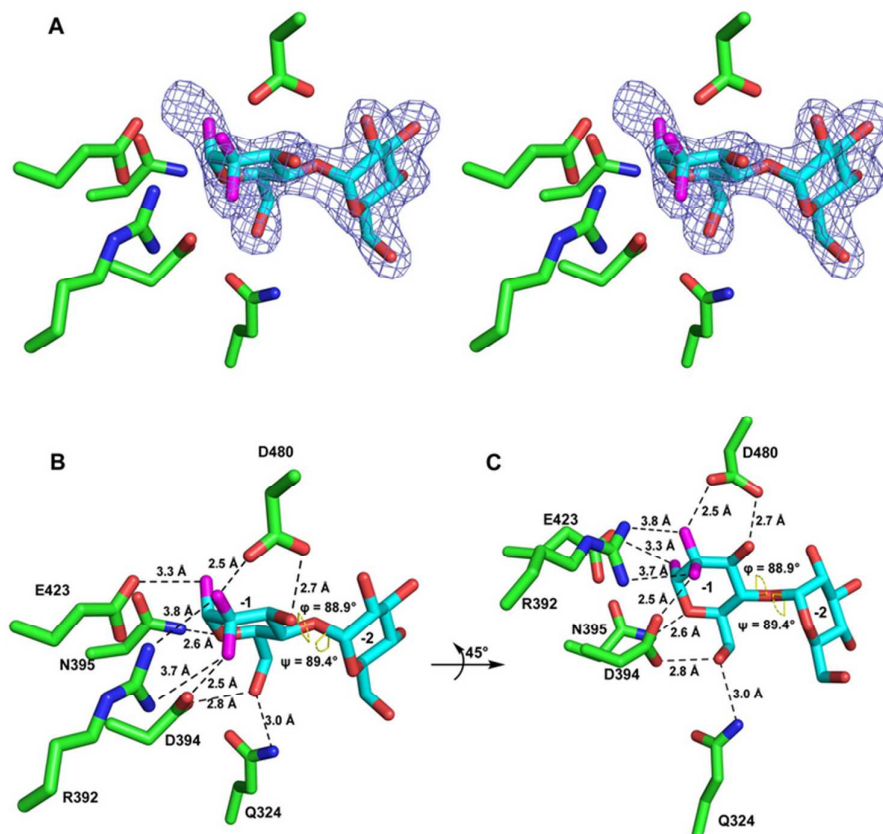


Fig 2. *Sco* GlgEI-V279S in complex with α -MTF. (A) Stereo, $|F_o - F_c|$ omit map calculated while omitting α -MTF is contoured at 3σ showing α -MTF bound in the enzyme active site. No covalently modified residue was observed in the crystal structure. Density is observed for the 2,2-difluoromethylene group at C2', which hydrogen bond with R392. (B)(C) The nucleophile, D394, appears to be forming a hydrogen bond with the equatorial fluorine at C2', suggesting that it may be protonated in this form. Glu423 appears to be forming a hydrogen bond with the C1' fluorine as Glu423 is expected to be protonated during the first step of catalysis. Hydrogen bonding distances from between donor and acceptor are indicated next to the dashed line.

immediately prior to nucleophilic attack without the need to disrupt catalytic residues. Further, comparison of the structure with other substrate analogues reveals how changes in analogue structure effect the organization of the active site residues and the conformation of the bound ligand.

Since α -MTF does not react with the GlgEI nucleophile in the α -MTF crystal structure, important information can be obtained and used in the design of inhibitors targeting *Sco* GlgEI and presumably the homologous *Mtb* GlgE. The presence of the difluoromethylene center on the C2' is resolved and forms a bidentate hydrogen bonding interaction with Arg392 in the active site. Despite the addition of two fluorine atoms at the C2' position, only minor alterations in the active site were observed in comparison *Sco* GlgEI-V279S-MCP complex, Fig. 3⁶. This suggests that the GlgE active site tolerates the inclusion of hydrogen bond acceptors at the axial C2' position and may indicate the site is tolerant of other modifications required to make future inhibitors more drug-like.

Comparison of the *Sco* GlgEI-V279S-MCP⁶ and *Sco* GlgEI-V279S- α -MTF at the -2 sugar binding subsite revealed identical

patters of hydrogen bonding within the active site (not shown). It was also notable that the Ser279 side chain forms a hydrogen bonding interaction with the endocyclic O5 atom in the -2 sugar binding subsite in both structures (also not shown). This observation reinforces our belief that the serine in the active site of *Mtb* GlgE is important for substrate recognition and would therefore affect inhibitor binding as well. Comparison of the *Sco* GlgEI-V279S- α -MTF (Fig. 3A) and *Sco* GlgEI-V279S-MCP (Fig. 3B) -1 sugar binding subsite site revealed more interesting changes. We noted identical patterns of potential hydrogen bonding for the Gln324 side chain with the O6'(H) (3.0 Å and 2.9 Å, measured between heteroatoms, respectively). Similarly, the Asp394 side chain oxygen shows possible hydrogen bonding with O6'(H) (2.8 Å measured between heteroatoms in both structures). The Asn395 side chain nitrogen is within similar hydrogen bonding distance of the endocyclic O5' atom (2.6 Å and 2.8 Å, respectively) in both structures as well. As mentioned previously, the α -MTF forms a bidentate hydrogen bonding interaction with the NH₁ and NH₂ side chain groups of Arg392

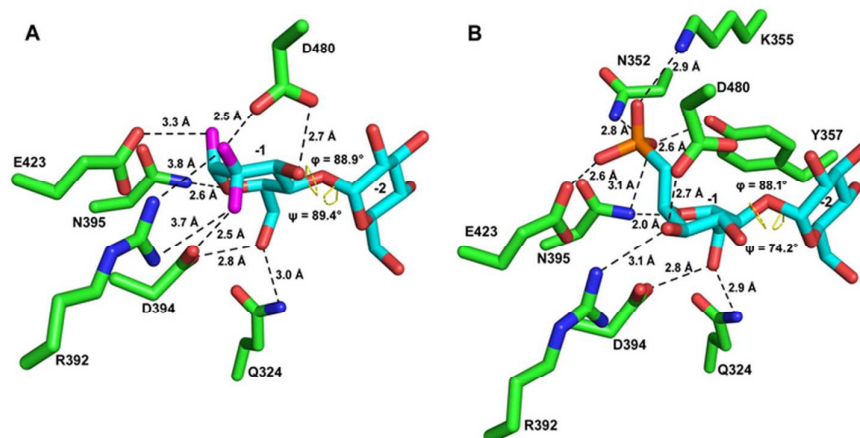


Fig 3. Comparison of the *Sco* GlgEI-V279S- α -MTF and *Sco* GlgEI-V279S-MCP complexes at the M1P binding site.

in the active site (3.8 Å and 3.7 Å). In contrast, the NH₂ group of Arg392 forms a monodentate interaction with O2'(H) (3.1 Å) in the *Sco* GlgEI-V279S-MCP structure while the NH₁ group forms a 2.8 Å hydrogen bond with side chain of the nucleophile, Asp394. The elongated bonding distances between α -MTF and Arg392 can be accounted for by a change in the ϕ torsion angle in the α -MTF ($\phi = 88.9^\circ$ and $\psi = 89.4^\circ$) relative to the MCP ($\phi = 72.4^\circ$ and $\psi = 88.1^\circ$) in the respective complexes. We suggest that this 14.7° change in ϕ angle results from significant additional binding interactions afforded by the phosphonate moiety of MCP. These additional interactions may place torsional strain on the scissile bond in the M1P substrate, facilitating displacement of the leaving group. Another observation is that the saccharide in the -1 sugar binding subsite of the α -MTF complex is oriented in an ideal ⁴C₁ conformation. In contrast, the MCP complex shows the endocyclic oxygen at the -1 sugar binding subsite flattened out (closer to the reference plane) with respect to and ideal ⁴C₁ conformation. The flattening out of the endocyclic oxygen has been predicted to be part of a necessary transition state geometry required during catalysis. Thus, it can also be concluded that the additional binding interactions present in the MCP complex may be required to achieve the distorted, transition-state-like geometry observed in the MCP complex. As mentioned previously, a hydrogen bonding interaction is noted between putative proton donor Glu423 and the C1'F in α -MTF at 3.3 Å measured between heteroatoms. These interactions provide evidence that Glu423 functions as a proton donor in the first catalytic step leading to the glycosyl enzyme intermediate.

Experimental

Crystallization of the *Sco* GlgEI-V279S- α -MTF

The *Sco* GlgEI-V279S concentrated to 8.0 mg/mL (0.1% Abs value of 1.526) was used for crystallization experiments. Compound **5** was added to the GlgE to a final concentration of

17 mM. Crystals of *Sco* GlgEI-V279S- α -MTF were grown by the hanging-drop vapor diffusion method with the crystallization drops containing 2 μ L of protein solution and 2 μ L of well solution. Drops were equilibrated against 100 μ L of well solution containing 0.2 M sodium citrate pH 7.0 and 10 % PEG 3350. Ethylene glycol was added to a final concentration of 25 % to the drop prior to flash-cooling.

Diffraction experiments

X-ray diffraction experiments were carried out at the LS-CAT beamline at the Advanced Photon Source of Argonne National Labs, Argonne, IL. The *Sco* GlgEI-V279S- α -MTF structure was elucidated using diffraction data collected at a wavelength of 1.07819 Å. Diffraction data were integrated and scaled using HKL3000¹².

Structural Determination of the *Sco* GlgE-V279S- α -MTF

The *Sco* GlgEI-V279S- α -MTF structure used the *Sco* GlgEI-V279S-MCP structure (RCSB ascension number 4U31) as a model for rigid body refinement. Rigid body refinement, simulated annealing, positional and B-factor refinements were performed using PHENIX^{13, 14}. Manual refinement of the structure was performed using COOT¹⁵. The α -MTF ligand and ligand restraints were generated using eLBOW software in PHENIX¹⁶. Validation of the *Sco* GlgEI-V279S- α -MTF was performed using Molprobit¹⁷.

General methods

All starting material compounds were bought from Acros organics or Aldrich. Unless specified all the reaction were done under nitrogen atmosphere. Reactions were monitored by Thin-layer chromatography (TLC silica gel 60 F₂₅₄) and spots were observed by dipping in 5% H₂SO₄, Ceric ammonium molybdate (CAM) or *p*-Anisaldehyde and heated. All solvents used for reaction were purchased from Fisher, purified and dried by distillation and other standard procedures, and solvents for column chromatography are used as purchased. Purifications of compounds were done by liquid

chromatography (silica gel column chromatography) with silica (porosity 60Å, 230-400 mesh) from sorbent technology. ¹H NMR, ¹³C NMR, G-COSY and HMQC spectra were carried out using a Bruker Avance III 600 or Inova 600 spectrometers in Fourier transformation mode. ¹H-NMR and ¹³C- NMR were referenced to residual CDCl₃ peak at 7.27 ppm, and 77.16 ppm respectively. ¹⁹F-NMR spectra were obtained by using VXRS400 and Gemini200 spectrometer and referenced to CFCl₃ (0.0 ppm). High resolution mass spectroscopy (HRMS) was performed on a micro mass Q-TOF2 instrument.

2',3',4',6'-Tetra-O-acetyl-α-D-glucopyranosyl-(1,4)-3,6-di-O-acetyl-2-deoxy-2,2-difluoro-α/β-D-glucosyl fluoride/hydroxide (2, 3, 4)

Condition a. The starting material 2-fluoro maltal (**1**) (36.1 mg, 62.5 μmol) was dissolved in CH₃NO₂ (3.0 mL). To the solution was added Selectfluor® (44.0 mg, 124 μmol). The reaction was stirred at room temperature for 2 h until it turned clear. Then, a second proportion of Selectfluor® (80.0 mg, 0.248 μmol) was added and the reaction maintained for 12 h. The reaction was then heated to reflux and maintained for 1 h to ensure complete conversion. The solvent was removed under reduced pressure and the crude mixture purified by gravity column chromatography on silica gel. The combined yield for **2** + **3** + **4** was 61%. Elution with hexanes-acetone (8:2) afforded 2-deoxy-2,2-difluoro-α-maltosyl fluoride **2**. Yield: 21% (8.1 mg); silica gel TLC *R_f* = 0.41 (7:3 hexanes-acetone). Compound **3**, 2-deoxy-2,2-difluoro-β-maltosyl fluoride. Yield: 18.5% (7.1 mg); silica gel TLC *R_f* = 0.42 (7:3 hexanes-acetone). Compound **4**, 2-deoxy-2,2-difluoro maltose hemiacetal. Yield: 21% (8.2 mg). Compound 2-deoxy-2,2-difluoro maltose hemiacetal **4** was scaled up (40.0 mg, 65.1 μmol) and treated with DAST to afford compounds **2** and **3**. Compound **4** was dissolved in dry DCM (4.0 mL) and cooled to -60 °C, and treated with DAST (41.0 mg, 130 μmol). The temperature of the reaction was allowed to rise to 0 °C and maintained for 2 h. The reaction was quenched with ice cold water and extracted with DCM (20 mL, 3 times). The organic layer was washed with NaHCO₃ (20.0 mL), and brine solution (20.0 mL). The DCM layer was dried over anhydrous Na₂SO₄ and concentrated under reduced pressure. The products were purified by gravity column chromatography on silica gel to obtain compounds **2** and **3** (1:1.1). Yield: 17% (7.0 mg). 2-deoxy-2,2-difluoro-α-maltosyl fluoride **2**: ¹H NMR (600 MHz, CDCl₃): δ 5.66-5.60 (m, 1H, H-3), 5.53 (d, 1H, ²*J*_{1,F} 50.62 Hz, H-1), 5.46 (d, 1H, ³*J*_{1,2'} 4.03 Hz, H-1'), 5.36 (dd, 1H, ³*J*_{3,2'} 10.27 Hz, ³*J*_{3,4'} 9.90 Hz, H-3'), 5.09 (t, 1H, *J* 9.90 Hz, H-4'), 4.87 (dd, 1H, ³*J*_{2,3'} 10.64 Hz, ³*J*_{1,2} 4.03 Hz, H-2'), 4.61 (dd, 1H, ²*J*_{6a,6b} 12.10 Hz, ³*J*_{6a,5} 1.47 Hz, H-6a), 4.27-4.25 (m, 2H, H-6a', H-6b'), 4.23 (m, 1H, H-5), 4.20-4.17 (m, 1H, H-4), 4.07 (dd, 1H, ²*J*_{6a,6b} 12.47 Hz, ³*J*_{6b,5} 2.20 Hz, H-6b'), 3.96-3.93 (m, 1H, H-5'), 2.18 (s, 3H, CH₃), 2.17 (s, 3H, CH₃), 2.12 (s, 3H, CH₃), 2.08 (s, 3H, CH₃), 2.04 (s, 3H, CH₃), 2.02 (s, 3H, CH₃) ppm; ¹³C-NMR (CDCl₃): δ 170.77 (C=O), 170.66 (C=O), 170.42 (C=O), 170.01 (C=O), 169.57 (C=O), 169.49 (C=O), 1.03.50-101.98 (¹*J*_{C1,F} 232.18 Hz, C1), 95.94 (C1'), 71.12 (C5), 70.85 (C2'), 70.35 (C2), 70.124 (C3), 69.29 (C3'), 68.90 (C5'), 67.95 (C4'), 61.72

(C6), 61.44 (C6'), 20.89 (CH₃), 20.83 (CH₃), 20.79 (CH₃), 20.75 (CH₃), 20.73 (2 CH₃) ppm; ¹⁹F-NMR: (Vxrs400 MHz, CDCl₃): δ -122.58 (m, 2F, Fa, Fe), -148.25 (d, 1F, ²*J*_{F1,H1} 50.98 Hz, F1) ppm; *m/z* = 639.1493 (M+Na)⁺, C₂₄H₃₁F₃O₁₅ requires 639.1513. 2-deoxy-2,2-difluoro-β-maltosyl fluoride (**3**): ¹H NMR (600 MHz, CDCl₃): δ 5.35 (dd, 1H, ¹*J*_{F1-1} 52.8 Hz, ³*J*_{F2a-1} 5.4 Hz, H-1), 5.42 (d, 1H, ³*J*₁₋₂ 4.2 Hz, H-1'), 5.39 (t, 1H, ³*J*_{3,2'} 10.2 Hz, H-3'), 5.29 (dd, 1H, ³*J*_{3,4'} 9.3 Hz, ³*J*_{3,4} 7.2 Hz, H-3), 5.08 (dd, 1H, ³*J*_{3,4'} 10.2 Hz, ³*J*_{4,5'} 9.2 Hz, H-4'), 4.85 (dd, 1H, ³*J*_{2,3'} 10.8 Hz, ³*J*_{2,1'} 4.2 Hz, H-2'), 4.59 (dd, 1H, ²*J*_{6a,6b} 12.10 Hz, ³*J*_{6a,5} 4.40 Hz, H-6a), 4.26 (dd, 1H, ²*J*_{6a,6b} 12.47 Hz, ³*J*_{6a,5} 4.03 Hz, H-6a'), 4.23 (dd, 1H, ²*J*_{6a,6b} 11.74 Hz, ³*J*_{6b,5} 4.77 Hz, H-6b), 4.21-4.19 (m, 1H, H-4), 4.15-4.13 (m, 1H, H-5), 4.08 (dd, 1H, ³*J*_{6a,6b} 12.47 Hz, ³*J*_{5,6'a} 2.4 Hz, H-6b'), 3.98-3.96 (m, 1H, H-5'), 2.18 (s, 3H, CH₃), 2.15 (s, 3H, CH₃), 2.11 (s, 3H, CH₃), 2.07 (s, 3H, CH₃), 2.04 (s, 3H, CH₃), 2.02 (s, 3H, CH₃) ppm; ¹³C-NMR (CDCl₃): δ 170.68 (C=O), 170.65 (C=O), 170.44 (C=O), 179.09 (C=O), 169.61 (C=O), 169.46 (C=O), 103.64-101.93 (d, *J*_{F,C1} 257.49 Hz, C1), 95.84 (C1'), 73.08 (C5), 71.35 (C4), 70.37 (C3), 69.46 (C3', C2'), 68.73 (C5'), 68.09 (C4'), 62.58 (C6), 61.56 (C6'), 20.88 (CH₃), 20.81 (CH₃), 20.78 (CH₃), 20.74 (CH₃), 20.67 (2CH₃) ppm; ¹⁹F-NMR (Vxrs400 MHz, CDCl₃): δ -114.63 (dd, 1F, ²*J*_{F,Fa} 285.2 Hz, ³*J*_{Fa,H1} 11.2 Hz, Fa), -127.74 (dd, 1F, *J*_{F,Fe} 285.6 Hz, Fe), -145.35 (dd, 1F, ²*J*_{F1,1} 54.8 Hz, ³*J*_{F1,Fa} 13.00 Hz, 1F) ppm; *m/z* = 639.1513 (M+Na)⁺, C₂₄H₃₁F₃O₁₅ requires 639.1507. 2-deoxy-2,2-difluoro maltose hemiacetal (**4**): ¹H NMR (600 MHz, CDCl₃): δ 5.68-5.63 (ddd, 1H, ³*J*_{Fa,3} 21.0 Hz, ³*J*_{3,4} 9.28 Hz, ⁴*J*_{3,1} 3.17 Hz, H3), 5.46 (d, 1H, ²*J*_{1,2'} 3.96 Hz, H-1'), 5.37 (dd, 1H, ³*J*_{3,2'} 10.25 Hz, ³*J*_{3,4'} 10.01 Hz, H-3'), 5.21 (s, 1H, H-1), 5.09 (t, 1H, ³*J*_{3,4'} 10.01 Hz, H-4), 4.87 (dd, 1H, ³*J*_{2,3'} 10.01 Hz, ³*J*_{2,1'} 3.91 Hz, H-1'), 4.56 (dd, 1H, ²*J*_{6a,6b} 12.45 Hz, ³*J*_{6a,5} 2.20 Hz, H-6a), 4.32-4.30 (m, 1H, H-5), 4.27 (dd, 1H, ²*J*_{6'a,6'b} 12.45 Hz, ³*J*_{6'a,5'} 3.42 Hz, H-6a'), 4.24 (dd, 1H, ²*J*_{6'a,6'b} 12.21 Hz, ³*J*_{6b,5} 3.66 Hz, H-6b), 4.13 (t, 1H, ³*J*_{3,4} 9.52 Hz, H4), 4.07 (dd, 1H, ²*J*_{6'a,6'b} 12.45 Hz, ³*J*_{6'b,5} 1.71 Hz, H-6b'), 3.98-3.96 (m, 1H, H-5'), 3.78 (s, 1H, OH), 2.16 (s, 3H, CH₃), 2.17 (s, 3H, CH₃), 2.11 (s, 3H, CH₃), 2.07 (s, 3H, CH₃), 2.04 (s, 3H, CH₃), 2.02 (s, 3H, CH₃) ppm; ¹³C-NMR (CDCl₃): δ 170.82 (C=O), 170.77 (2 C=O), 170.14 (C=O), 169.77 (C=O), 169.63 (C=O), 115.51 (dd, ¹*J*_{C2',F} 257.145 Hz, ¹*J*_{C2',F} 242.59 Hz, C2), 95.73 (C1'), 91.09 (dd, ²*J*_{F,1} 35.50 Hz, ²*J*_{F,1} 27.99 Hz, C1), 71.78 (d, ³*J*_{F,4} 5.83 Hz, C4), 70.83 (dd, ²*J*_{F,3} 19.18 Hz, ²*J*_{F,3} 18.78 Hz, C3), 70.23 (C2'), 69.43 (C2), 68.70 (C5), 68.67 (C5'), 68.05 (C4'), 62.51 (C6), 61.51 (C1'), 20.98 (CH₃), 20.89 (CH₃), 20.84 (CH₃), 20.77 (CH₃), 20.74 (2 CH₃) ppm; ¹⁹F-NMR: (Vxrs400 MHz, CDCl₃): δ -120.84 (dd, 1F, ²*J*_{Fa,Fe} 251.77 Hz, ³*J*_{Fa,3H} 3.05 Hz, Fa-2), -122.81 (dd, ²*J*_{Fa,Fe} 251.77 Hz, ³*J*_{Fa,3H} 19.84 Hz, Fe-2) ppm; *m/z* = 639.1556 (M+Na)⁺, C₂₄H₃₂F₂O₁₆ requires 639.1556.

α-D-glucopyranosyl-(1,4)-2-deoxy-2,2-difluoro-α-D-glucopyranosyl fluoride (5)

Compound **2** (8.6 mg) was dissolved in MeOH (1.5 mL) and the solution cooled to -10 °C using dry ice in acetone. Ammonia gas was bubbled into the cooled solution for 10 min. The outlet of the reaction apparatus was connected to a bent finger trap cooled to -78 °C to trap any escaping ammonia gas. The reaction was maintained at room temperature for 2 h. The

reaction was concentrated to obtain an oily liquid of crude compound **5**. This compound was dissolved in a minimum amount of H₂O and purified by C-18 chromatography (2% methanol in H₂O), to obtain pure compound **5**. ¹H NMR (600 MHz, CD₃OD): δ 5.62 (dd, 1H, ¹J_{F1-1} 51.3 Hz, ³J_{F2a-1} 5.6 Hz, H-1) 5.30 (d, 1H, ³J₁₋₂ 3.8 Hz, H-1'), 4.24-4.18 (m, 1H, H-3), 3.94 (m, 1H, H-4), 3.90-3.82 (m, 4H, H-6a', H-6b, H-5, H-6a), 3.68-3.64 (m, 2H, H-5', H-6a), 3.61 (dd, 1H, ³J_{3',2'} 9.35 Hz, ³J_{3',4'} 9.35 Hz, H-3'), 3.44 (dd, 1H, ³J_{2',3'} 9.72 Hz, ³J_{1,2} 3.61 Hz, H-2'), 3.26 (dd, 1H, ³J_{3',4'} 9.54 Hz, ³J_{4',5'} 9.17 Hz, H-4') ppm; ¹³C-NMR (CD₃OD) : δ 118.33-114.78 (m, 1C, C2), 106.21-105.73 (ddd, ¹J_{F1,C1} 226.68 Hz, ²J_{F2a,C1} 40.71 Hz, ²J_{F2e,C1} 31.91 Hz, C1), 102.51 (C1'), 77.44 (d, ⁴J_{F,C4} 7.74, C4), 75.52 (C5), 75.17 (C5'), 75.12 (C3'), 74.23 (C2'), 72.14 (dd, ²J_{F2a,C3} 19.81 Hz, ²J_{F2e,C3} 18.71 Hz, C3), 71.76 (C4'), 62.93 (C6), 61.31 (C6') ppm; ¹⁹F-NMR (Gemini 200MHz, MeOD): δ -120.33 (ddd, 1F, ²J_{Fe,Fa} 280.77 Hz, ³J_{Fa, F1} 12.21 Hz, ³J_{Fa, H1} 6.10 Hz, Fa), -123.34 (dd, 1F, ¹J_{Fe,Fa} 262.46 Hz, Fe), -144.79 (m, 1F, ²J_{F1,H1} 48.83 Hz, 1F) ppm; Mass spectrum (HRMS), *m/z* = 387.0876 (M+Na)⁺, C₁₂H₁₉F₃O₆ requires 387.0876.

α-D-glucopyranosyl-(1,4)-2-deoxy-2,2-difluoro-β-D-glucopyranosyl fluoride (6)

Compound **3** (8.6 mg) was dissolved in MeOH (1.5 mL) and solution cooled to -10 °C using dry ice in acetone. Ammonia gas was bubbled into the solution for 10 min. The outlet of the reaction apparatus was connected to a bent finger trap cooled to -78 °C to trap any escaping ammonia gas. The reaction was maintained at room temperature for 2 h. The reaction was concentrated to obtain an oily liquid of crude compound **6**. The crude compound was dissolved in minimum amount of H₂O and purified by C-18 chromatography (2% methanol in H₂O), to obtain pure compound **6**; ¹H NMR (600 MHz, CD₃OD): δ 5.47 (dd, 1H, ¹J_{F1-1} 50.2 Hz, ³J_{F2a-1} 13.02 Hz, H-1), 5.29 (d, 1H, ³J₁₋₂ 3.8 Hz, H-1'), 4.11-4.05 (m, 1H, H-3), 3.92 (dd, 1H, ²J_{6'a,6'b} 12.47 Hz, ³J_{6'b,5} 2.02 Hz, H-6b'), 3.87-3.82 (m, 3H, H-4, H-6b, H-6a') 3.67-3.63 (m, 3H, H-5', H-5, H-6a), 3.58 (dd, 1H, ³J_{3',2'} 9.35 Hz, ³J_{3',4'} 9.35 Hz, H-3'), 3.44 (dd, 1H, ³J_{2',3'} 9.72 Hz, ³J_{1,2} 3.85 Hz, H-2'), 3.27 (dd, 1H, ³J_{3',4'} 9.35 Hz, ³J_{4',5'} 9.17 Hz, H-4') ppm; ¹³C-NMR (CD₃OD) : δ 117.86-114.37 (m, 1C, C2), 105.90-104.11 (ddd, ¹J_{F1,C1} 220.08 Hz, ²J_{F2a,C1} 30.81 Hz, ²J_{F2e,C1} 19.81 Hz, C1), 102.16 (C1'), 77.42 (d, ⁴J_{F,C4} 6.60 Hz, C4), 76.90 (d, ¹J_{F,C5'} 3.30 Hz, C5), 75.08 (C5'), 75.06 (C3'), 74.36 (dd, ²J_{F2a,C3} 18.71 Hz, ²J_{F2e,C3} 18.71 Hz, C3), 74.01 (C2'), 71.61 (C4'), 62.83 (C6), 61.63 (C6') ppm; ¹⁹F-NMR (Gemini 200MHz, MeOD): δ -121.51 (ddd, 1F, ²J_{Fe,Fa} 245.68 Hz, ³J_{Fa, F1} 15.26 Hz, ³J_{Fe, H1} 6.10 Hz, Fa), -138.585 (m, 1F, ¹J_{Fe,Fa} 245.67 Hz, Fe), -157.62 (ddd, 1F, ²J_{F1,H1} 50.35 Hz, ³J_{F1, Fa} 15.26 Hz, ³J_{F1, Fe} 10.68 Hz, 1F) ppm; Mass spectrum (HRMS), *m/z* = 387.0873 (M+Na)⁺, C₁₂H₁₉F₃O₆ requires 387.0879.

Inhibition studies

The procedure for this assay is previously reported.⁴ The assay is performed at room temperature using a Spectra max 340PC microplate reader and a 96 well transparent plate. Each reaction mixture contains 1 mM MESG (20 μL), 0.2 U of PNP (1

μL), 20X reaction buffer (1.0 M Tris-HCl, 20 mM MgCl₂, PH 7.5, containing 2 mM sodium azide) (5 μL), 50 nM *Sco* GlgE1-V279S (5 μL), 250 μM sodium salt of α-maltosyl-1-phosphate (3.125 μL), and glycogen (5 μL). Using deionized H₂O varied concentrations (0.1 to 10 mM) of inhibitor solutions were diluted from a 50 mM stock solution of inhibitor **5** (50 μM). Deionized water was added to bring the final reaction volume to 100 μL. For the positive control, inhibitor **5** was not included in the reaction. For the negative control, *Sco* GlgE1-V279S was not added to the reaction. The initial velocity of the reactions with and without inhibitor was used to calculate the percent inhibition (V_i'/V_i), where V_i' = initial velocity of reaction with inhibitor and V_i = initial velocity of reaction without inhibitor. The inhibitor showed no inhibition ($V_i'/V_i = 1$).

¹⁹F-NMR

(VXRS 400 MHz, CFCl₃ = 0 ppm): ¹¹ The reaction is carried out in a capillary NMR tube inserted into 5 mm NMR tube with D₂O. The D₂O present in the external tube was used to shim and lock the instrument. The reaction mixture contained glycogen (0.5 μL), 20X reaction buffer (1.0 M Tris-HCl, 20 mM MgCl₂, PH 7.5, containing 2mM sodium azide), compound **5** 1 mM (1.5 μL), *Sco* GlgE1-V279S 50 nM (2.5 μL). The reaction mixture was diluted up to 500 μL using deionized water. ¹⁹F-NMR were recorded at an intervals of 5 min, 10 min, 20 min, 30 min, 1h, 2h, and 10 h.

MS labeling studies

A stock solution of 2-deoxy-2,2-difluoro-α-maltosyl fluoride (**5**) at a concentration of 130 μM was added to a solution of 13 μM *Sco* GlgE1-V279S (1 mg/mL) in ammonium acetate pH 7.0. The reaction mixture was incubated at room temperature for 2 h. The excess of compound **5** was removed using 3 buffer exchange steps into a 10 mM ammonium acetate pH 7.0 buffer using ultrafiltration. The protein samples were digested with sequencing-grade trypsin using standard protocols (Promega). Determination of peptide mass was carried out by MALDI-MS using a Bruker UltrafleXtreme (Bruker Daltonics). The mass of only the native protein fragment was observed (*m/z* = 1695.9020).

Sco-GlgE-V279S maltooligosaccharide extension using M1F and α-MTF as substrates

Enzymatic reactions were carried out in 50 μL reactions containing 50 nM of GlgE and 1 mM maltohexaose in a reaction solution containing 20 mM sodium acetate at pH 7.5. Four reactions were performed: a control containing only maltohexaose (M6), a control reaction of only GlgE and M6, a reaction containing GlgE, M6, and 1 mM of M1F, and a final reaction containing GlgE, M6 and 1 mM of the α-MTF.

Determination of maltooligosaccharide size using MALDI-MS

One μL aliquots of each reaction were removed after 10 minutes and the reactions quenched using 19 μL of a saturated

DHB (2,5-dihydroxybenzoic acid) matrix solution dissolved in acetonitrile/water (1:1, v/v) with 0.1% trifluoroacetic acid (TFA). Determination of maltooligosaccharide elongation was carried out in positive-ion reflectron mode using an UltrafleXtreme MALDI-TOF/TOF mass spectrometer (Bruker).

Conclusions

In summary, we have synthesized 2-deoxy-2,2-difluoro- α -maltosyl fluoride (**2**), and the epimeric 2-deoxy-2,2-difluoro- β -maltosyl fluoride (**3**) in a single step from peracetylated 2-fluoro-maltal **1** using Selectfluor[®]. Trifluoride **2** was successfully deprotected to afford α -MTF, a non-hydrolysable substrate mimic of M1P. Enzymatic, mass spectral, and ¹⁹F-NMR studies with *Sco* GlgEI-V279S showed no inhibition at concentrations below 10 mM, no labeled protein, and no fluoride release, respectively. The lack of significant inhibition by α -MTF suggests both that the phosphate and equatorial OH moieties in M1P contribute significantly to substrate binding. This data also suggest that the role of the -2 sugar binding subsite is primarily shape recognition. The unreactive nature of α -MTF supports the notion that *Sco* GlgEI-V279S likely proceeds through a late dissociate transition state, destabilized by the 2,2-fluoromethylene modification, in the first step of the enzymatic reaction.¹⁸ The X-ray structure of the *Sco* GlgEI-V279S in complex with α -MTF was solved. These results also illustrate how *Sco* GlgEI-V279S can be used *in lieu of Mtb* GlgE to rapidly probing important protein-ligand interactions. In these studies α -MTF was found to be useful as probe molecule for interrogating key active site binding interactions. When these interactions are compared in conjunction with the MCP complex, the role of the phosphate in M1P on binding conformation can be inferred. The combined structural data from the α -MTF and MCP complexes will inevitably be helpful in the design potent inhibitors of the homologue *Mtb* GlgE enzyme, a genetically validated target for TB treatment.

Acknowledgements

This work was supported in part by a DeArce Memorial Fund grant to S. J. S. from The University of Toledo and a grant from the National Institutes of Health (grant number AI105084) to S.J.S and D. R. R.

Notes and references

1. W. H. Organization, 2014.
2. S. Pradhan, A. G. Mathur and A. Patil, *J. Drug Deliver. Ther.*, 2014, **4**, 69-73.
3. R. Kalscheuer, K. Syson, U. Veeraraghavan, B. Weinrick, K. E. Biermann, Z. Liu, J. C. Sacchettini, G. Besra, S. Bornemann and W. R. Jacobs, Jr., *Nat. Chem. Biol.*, 2010, **6**, 376-384.
4. S. K. Veleti, J. J. Lindenberger, D. R. Ronning and S. J. Sucheck, *Bioorg. Med. Chem.*, 2014, **22**, 1404-1411.
5. S. K. Veleti, J. J. Lindenberger, S. Thanna, D. R. Ronning and S. J. Sucheck, *J. Org. Chem.*, 2014, **79**, 9444-9450.

6. J. J. Lindenberger, S. K. Veleti, B. N. Wilson, S. J. Sucheck and D. R. Ronning, *Sci. Reports (manuscript has been reviewed as acceptable with minor revision see material for review but not publication)* 2015.
7. K. Syson, C. E. Stevenson, M. Rejzek, S. A. Fairhurst, A. Nair, C. J. Bruton, R. A. Field, K. F. Chater, D. M. Lawson and S. Bornemann, *J. Biol. Chem.*, 2011, **286**, 38298-38310.
8. K. Syson, C. E. Stevenson, A. M. Rashid, G. Saalbach, M. Tang, A. Tuukkanen, D. I. Svergun, S. G. Withers, D. M. Lawson and S. Bornemann, *Biochemistry*, 2014, **53**, 2494-2504.
9. C. Braun, G. D. Brayer and S. G. Withers, *J. Biol. Chem.*, 1995, **270**, 26778-26781.
10. R. Zhang, J. D. McCarter, C. Braun, W. Yeung, G. D. Brayer and S. G. Withers, *J. Org. Chem.*, 2008, **73**, 3070-3077.
11. M. Braitsch, H. Kahlig, G. Kontaxis, M. Fischer, T. Kawada, R. Konrat and W. Schmid, *Beilstein J. Org. Chem.*, 2012, **8**, 448-455.
12. Z. Otwinowski and W. Minor, *Method Enzymol.*, 1997, **276**, 307-326.
13. P. V. Afonine, R. W. Grosse-Kunstleve, N. Echols, J. J. Headd, N. W. Moriarty, M. Mustyakimov, T. C. Terwilliger, A. Urzhumtsev, P. H. Zwart and P. D. Adams, *Acta Crystallogr., Sect. D: Biol. Crystallogr.*, 2012, **68**, 352-367.
14. P. D. Adams, P. V. Afonine, G. Bunkoczi, V. B. Chen, I. W. Davis, N. Echols, J. J. Headd, L. W. Hung, G. J. Kapral, R. W. Grosse-Kunstleve, A. J. McCoy, N. W. Moriarty, R. Oeffner, R. J. Read, D. C. Richardson, J. S. Richardson, T. C. Terwilliger and P. H. Zwart, *Acta Crystallogr., Sect. D: Biol. Crystallogr.*, 2010, **66**, 213-221.
15. P. Emsley, B. Lohkamp, W. G. Scott and K. Cowtan, *Acta Crystallogr. Sect. D: Biol. Crystallogr.*, 2010, **66**, 486-501.
16. N. W. Moriarty, R. W. Grosse-Kunstleve and P. D. Adams, *Acta Crystallogr., Sect. D: Biol. Crystallogr.*, 2009, **65**, 1074-1080.
17. V. B. Chen, W. B. Arendall, 3rd, J. J. Headd, D. A. Keedy, R. M. Immormino, G. J. Kapral, L. W. Murray, J. S. Richardson and D. C. Richardson, *Acta Crystallogr. Sect. D: Biol. Crystallogr.*, 2010, **66**, 12-21.
18. G. Speciale, A. J. Thompson, G. J. Davies and S. J. Williams, *Curr. Opin. Struct. Biol.*, 2014, **28**, 1-13.